Inorganic Chemistry

pubs.acs.org/IC

Article

Next-Generation 3,3′-AlkoxyBTPs as Complexants for Minor Actinide Separation from Lanthanides: A Comprehensive Separations, Spectroscopic, and DFT Study

Lesta S. Fletcher, Mariah L. Tedder, Samiat O. Olayiwola, Nickolas A. Joyner, Marcos M. Mason, Allen G. Oliver, Dale D. Ensor, David A. Dixon, and Jesse D. Carrick*

Cite This: *Inorg. Chem.* 2024, 63, 4819−4827

Read Online

ACCESS | Metrics & More | Article Recommendations | Supporting Information

ABSTRACT: Progress toward the closure of the nuclear fuel cycle can be achieved if satisfactory separation strategies for the chemoselective speciation of the trivalent actinides from the lanthanides are realized in a nonproliferative manner. Since Kolarik's initial report on the utility of bis-1,2,4-triazinyl-2,6-pyridines (BTPs) in 1999, a perfect complexant-based, liquid−liquid separation system has yet to be realized. In this report, a comprehensive performance assessment for the separation of $^{241}Am^{3+}$ from $^{154}Eu^{3+}$ as a model system for spent nuclear fuel using hydrocarbon-actuated alkoxy-BTP complexants is described. These newly discovered complexants realize gains that contemporary aryl-substituted BTPs have yet to achieve, specifically: long-term stability in highly concentrated nitric acid solutions relevant to the low pH of unprocessed spent nuclear fuel, high D_{Am} over D_{Eu} in the economical, nonpolar diluent Exxal-8, and the demonstrated capacity to complete the separation cycle with high efficiency by depositing the chelated An^{3+} to the aqueous layer via decomplexation of the metal−ligand complex. These soft-N-donor BTPs are hypothesized to function as bipolar complexants, effectively traversing the organic/aqueous interface for effective chelation and bound metal/ligand complex solubility. Complexant design, separation assays, spectroscopic analysis, single-crystal X-ray crystallographic data, and DFT calculations are reported.

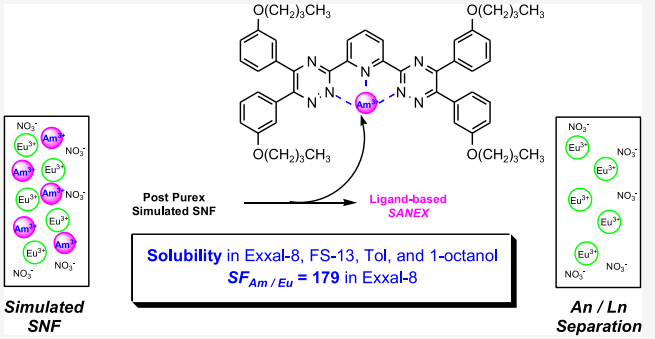

INTRODUCTION

Widely accepted as a carbon-neutral form of energy, nuclear fission will maintain its status as a significant contributor to the energy portfolio of the world well into the 21st century. The ever-burgeoning volume of spent nuclear fuel (SNF) from legacy waste and civilian energy production continues to threaten environmental security. Complete closure of the nuclear fuel cycle is predicated, at least in part, on an effective process to recycle, or transmutate, the post PUREX transuranic minor An, specifically $^{241}Am^{3+}$ and $^{244}Cm^{3+}$,[1] found in SNF, to isotopes with shorter half-lives, lower radiotoxicity, and a decreased heat load for storage in a geologic repository.[2] Any suitable strategy for recycling the minor An to fast-neutron reactors must first include chemoselective separation from the neutron-poisoning lanthanides,[3] also produced as byproducts of nuclear fission. Similar physical properties including oxidation state, cationic radius, hardness, and complexation behavior, render the aforementioned a grand challenge in separation science. Over the previous three decades, liquid−liquid separation strategies have demonstrated some success in the separation of minor An from Ln in simulated SNF, although substantive challenges remain.

In 1999, Kolarik disclosed that soft-N-donor, alkyl substituted, and tridentate Lewis basic complexants of the bis-1,2,4-triazinyl-2,6-pyridine (BTP) class could effectively speciate $^{241}Am^{3+}$ from $^{154}Eu^{3+}$ from SNF in liquid−liquid separations assays (Figure 1).[4] Preliminary complexants of this class possessed several challenges, including slow complexation kinetics and oxidative degradation at the pseudobenzylic position of the 5,6-dialkyl substituted-1,2,4-triazine, in addition to susceptibility to radiolytic degradation. Other applications of BTPs in An separations have also been disclosed.[5] Complexants incorporating different Lewis basic cores, including 2,2′-bipyridine-2,6-bis-carbonitrile[6] or 1,10-phenanthroline-2,6-bis-carbonitrile[7] have been prepared and evaluated in separation assays with congruent, and sometimes improved performance over traditionally symmetric BTPs.[8] Complexants for hydro-

Received: June 21, 2023
Revised: January 31, 2024
Accepted: February 1, 2024
Published: March 4, 2024

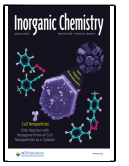

https://doi.org/10.1021/acs.inorgchem.3c02061
Inorg. Chem. 2024, 63, 4819−4827

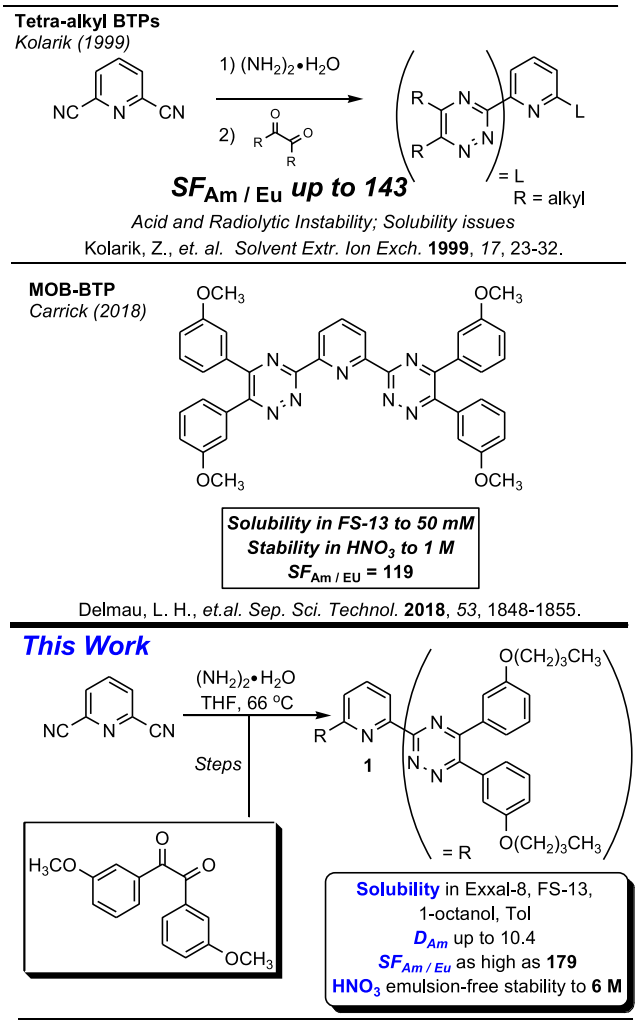

Figure 1. Summary of BTPs studied in liquid−liquid separations of minor An from Ln.

philic separations discretely,[9] or in concert with other separation strategies,[10] as well as resin-bound applications[11] have also been reported.

In 2016, Carrick disclosed a unified synthetic approach to the BTP class of complexants, leveraging a bis-hydrazonimide telescoped condensation strategy to afford aryl-functionalized BTPs.[12] Further efforts saw the development of Pd-catalyzed amination[13] and Suzuki−Miyaura cross-coupling[14] methods to modulate the physical properties of BTP complexants and related synthons. Additional synthetic methodologies providing access to unsymmetric[15] and frustrated[16] BTP-type complexants were also realized (Figure 1). Follow-up studies using density functional theory (DFT) have defined important computational parameters for the chemoselective speciation of the minor An over Ln,[17] in addition to the effects of metal hydration on separations.[18] One of the underlying hypotheses for this initial work centered on the concept of improving the solubility of the BTP, a polar molecule, in nonpolar diluents while simultaneously improving the hydro- and radiolytic stability by synthetically introducing an aromatic spacer at the 5,6-positions of the 1,2,4-triazine.

In 2018, a disclosure of 3,3′-dimethoxy-BTP (MOB-BTP)[19] highlighted the capacity to affect the desired minor An/Ln separation from simulated SNF at one-half the concentration, 25 mM, of a comparable European benchmark complexant, bis-2,6-(5,6,7,8-tetrahydro-5,9,9-trimethyl-5,8-methano-1,2,4-benzotriazin-3-yl)pyridine (CA-BTP), at 50 mM.[20] Interestingly, the 4,4′-dimethoxy-BTP was completely insoluble in trifluoromethyl phenyl sulfone (FS-13), whereas the constitutional isomer, MOB-BTP, was soluble to 50 mM, possessed stability in aqueous HNO_3 to 2 M, and afforded an Am/Eu Separation Factor (*SF*) 119. Solubility in nonpolar diluents remained a challenge with this complexant. Encouraged by the performance advantages offered by MOB-BTP over CA-BTP, especially regarding ease of synthetic preparation of one compound versus unregulated production of numerous diastereomers, effort focused on capitalizing on the BTP's tridentate core for chelation while leveraging the periphery[21] and dimensional topography of the complexant to improve solubility, stability, and chelation in nonpolar diluents.

In this article, an example of a new class of aryl-alkoxy BTPs soluble in Exxal-8,[22] which are hydrolytically stable in $HNO_{3(aq)}$ to 6 M with excellent distribution (D_M) values and *SF* for $^{241}Am^{3+}$ over $^{154}Eu^{3+}$ is described. These new complexants are hypothesized to have bipolar properties, where the nonpolar side chain and polar core synergistically complement each other to allow facile interfacial transfer of the minor An from the acidic aqueous phase to the organic layer. Synthetic access via a dealkylation/ligation/condensation strategy provided various 3,3′- and 4,4′-alkoxy-BTP congeners,[23] which were studied in liquid−liquid separation assays of simulated SNF. Single-crystal X-ray diffraction studies illuminated the solid-state bond lengths and angles, as well as the coordination number, while underscoring the role of the inner/outer sphere counterion stability of $^{241}Am^{3+}$. Analytical spectroscopy experiments involving UV−visible studies preliminarily assessed the metal−ligand coordination number beyond slope analysis. Evaluation of the stability of metal−ligand chelates at various hydration/substituent levels from DFT calculations showed that Am(III) binding is favored over Eu(III) binding when two ligands are present in the complex, or if nitrate is present, but not when only water is present in the inner coordination sphere. Separations, spectroscopic, and decomplexation data are reported herein.

EXPERIMENTAL SECTION

Chemicals. All reagents were purchased from U.S. chemical suppliers, stored according to published protocols, and used as received unless indicated otherwise.

Safety Considerations. Caution! The ^{241}Am and ^{154}Eu solutions used in this work were highly radioactive. All manipulation of these samples was performed in a dedicated radiological facility using well-established radiological safety protocols.

Solvent Extraction. *Organic Phase.* An appropriate mass of **1** was transferred from a sample vial to a Class A volumetric flask of 5.0 mL to make a concentrated stock solution. Weighing by difference was used on the original sample vial to calculate the actual mass of **1** dissolved. The diluent was added to the flask and manually agitated to facilitate dissolution. Generally, the complexant did not dissolve immediately and was left to sit for approximately 1 h. If the complexant was not fully dissolved after 1 h, the solution was sonicated for 5 min. Various concentrations of **1** were prepared from the concentrated stock solution in 1.0 or 2.0 mL of Class A volumetric glassware.

Aqueous Phase. Eight concentrated stock solutions of $^{241}Am^{3+}$ were prepared in various concentrations of HNO_3 (0.25−5.0 M). These $^{241}Am^{3+}$ stock solutions were used throughout this study to spike the working aqueous phase of matching [HNO_3]. Initial counts

https://doi.org/10.1021/acs.inorgchem.3c02061
Inorg. Chem. 2024, 63, 4819−4827

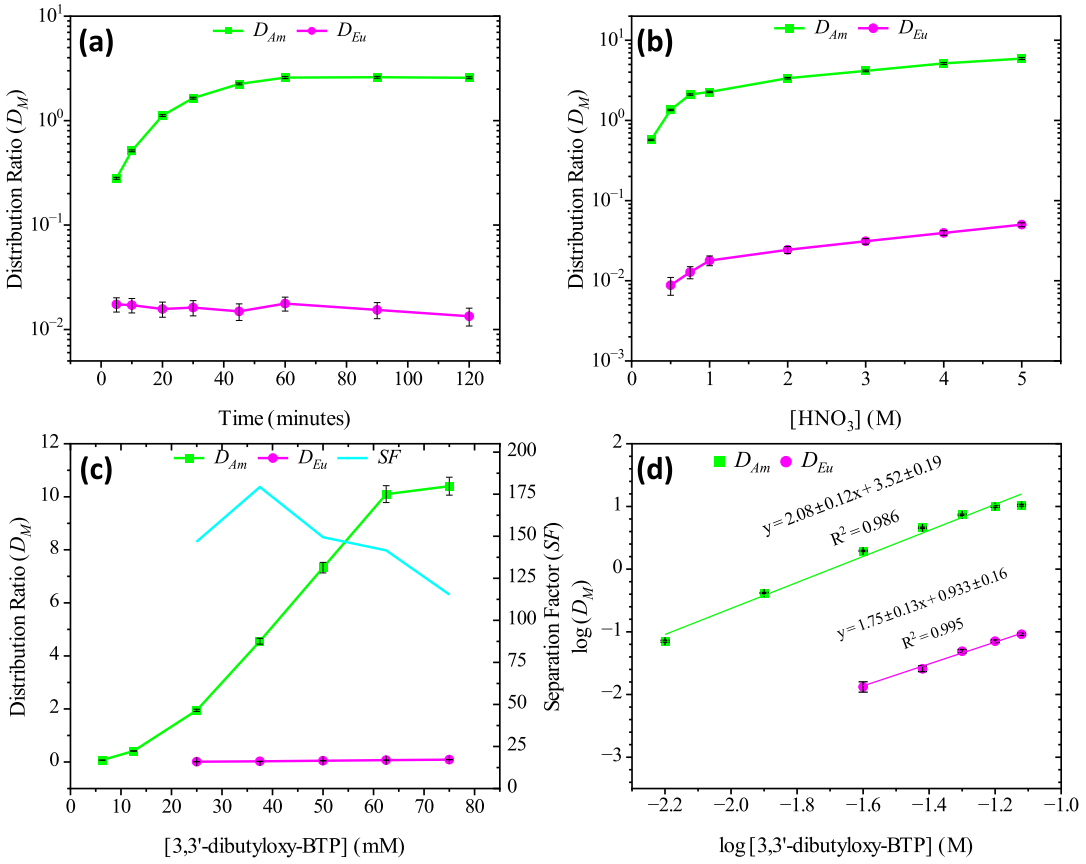

Figure 2. $^{241}Am^{3+}$ and $^{154}Eu^{3+}$ (D)- as a function of (a) contact time (organic phase: [Complexant **1**] = 25 mM dissolved in Exxal-8, aqueous phase: $[HNO_3]_{initial}$ = 1 M with $^{241}Am^{3+}$ and $^{154}Eu^{3+}$ tracers), (b) initial $HNO_{3(aq)}$ concentration; organic phase: [Complexant **1**] = 25 mM dissolved in Exxal-8, aqueous phase: $[HNO_3]_{initial}$ = 0.25−5 M with $^{241}Am^{3+}$ and $^{154}Eu^{3+}$ tracers, contact time = 1 h, (c) initial ligand concentration (organic phase: [Complexant **1**] = 6.25−75 mM dissolved in Exxal-8, aqueous phase: $[HNO_3]_{initial}$ = 1 M with $^{241}Am^{3+}$ and $^{154}Eu^{3+}$ tracers, contact time = 1 h, and (d) initial ligand concentration log−log plot.

of the aqueous phase were generally 3400 cpm/200 μL. This method was repeated for $^{154}Eu^{3+}$.

Extraction. Equal volumes (0.6 mL) of the organic and active aqueous phases, in that order, were added to a 1.5 mL microcentrifuge tube. Centrifuge tubes were capped and wrapped in the parafilm and then placed on a pulsing vortex shaker at 1700 rpm for the appropriate time. After the allotted time on the vortex shaker, the samples were centrifuged for five min to achieve phase separation. The organic and aqueous phases were transferred to separate 1.5 mL centrifuge tubes with a disposable fine-tip transfer pipet. A 200 μL aliquot of each phase was transferred to a counting tube, with sampling performed in duplicate.

Gamma Spectroscopy. A 2470 Wizard2 automatic gamma counter with a 3 inch NaI(Tl) source was used for the determination of the $^{241}Am^{3+}$ and $^{154}Eu^{3+}$ activity of the samples. Samples were counted for 10 min, or until total counts reached 10000, and the instrument software relayed the results as counts per minute (CPM). The distribution ratios of a given metal ion (D_M) were calculated according to eq 1, where metal concentration, [M], is the net CPM of either the organic phase (numerator) or aqueous phase (denominator). Separation factors (SF) were calculated using eq 2. Values are reported in figures as an average of duplicate samples, with error bars representing uncertainties calculated at 2σ from the counting error. The Supporting Information in this work provides further detail.

$$D_M = \frac{[M]org}{[M]aq} \quad (1)$$

$$SF_{Am(III)/Eu(III)} = \frac{D_{Am(III)}}{D_{Eu(III)}} \quad (2)$$

Decomplexation. An initial liquid−liquid extraction was performed following the method described above in the solvent extraction section, with the exception of volumes being increased from 600 to 800 μL. A 700 μL aliquot of the $^{241}Am^{3+}$-loaded organic phase was transferred to a new microcentrifuge tube, and an equal volume of HNO_3 was added. The concentration of HNO_3 was varied. The phases were contacted on a vortex mixer (1700 rpm) for 60 min, followed by 5 min of centrifugation. The phases were separated and analyzed following the method described in the solvent extraction section.

UV−vis Titration. UV−visible spectrophotometric titrations were performed in a 3 mL, 1.00 cm path length quartz cuvette using a Cary 5000 UV−vis spectrophotometer. For each titration, an appropriate volume of a 1.5 × 10^{-3} M $Ln(NO_3)_3$ (Ln = Nd, Eu, or Ho) solution in 99% acetonitrile/1% water (v/v) was added to 2.0 mL of a 1.5 × 10^{-5} M solution of **1** in the same solvent system. A wavelength scan from 225 to 450 nm at a scan rate of 100 nm per minute and a 5 data point average were taken of the free (uncomplexed) complexant after each titration. The sample was manually agitated for three min after each titration to ensure complete complexation. The titration was complete when the variation in the absorbance became negligible. Raw spectra were baseline corrected with OriginPro software and imported into HypSpec[28] software for the determination of stability constants by nonlinear regression curve fitting.

Single-Crystal X-ray Diffraction. A 1.00 mL, 4.81 × 10^{-2} M solution of $Nd(NO_3)_3$ (0.0211 g, 4.81 × 10^{-5} mol, 1.13 equiv) was prepared in acetonitrile/ethanol (0.9 mL CH_3CN, 0.1 mL EtOH-9.00:1.00 v/v, 0.03 M). A (1.00 mL, 4.26 × 10^{-2} M) solution of **1** (0.0353 g, 4.26 × 10^{-5} mol, 1.00 equiv) was prepared separately in acetonitrile. The solution of **1** was heated at 40 °C for two min for the

https://doi.org/10.1021/acs.inorgchem.3c02061
Inorg. Chem. 2024, 63, 4819−4827

complexant to completely dissolve. The $Nd(NO_3)_3$ solution was slowly added to the vial containing the 3,3-dibutyloxy-BTP, gently agitated, and left to sit for 1 week. After 1 week, the cap was punctured to facilitate the evaporation of the solvent over the course of 34 days to afford the crystalline material, which was used for crystallographic studies.

RESULTS AND DISCUSSION

Solvent Extraction Experiments. An equilibration study of **1** at 25 mM in 1 M $HNO_{3(aq)}$ was executed, resulting in the data disseminated in Figure 2a. Equilibration of this system in Exxal-8 was reached in 60 min with a D_{Am} = 2.6 for $^{241}Am^{3+}$. Further complexant contact time did not promote additional extraction with this diluent. The D_{Eu} range of 0.013−0.017 remained relatively constant throughout the analysis. With confirmation of the optimization contact time of 60 min observed, effort was focused on performing a $[HNO_{3(aq)}]$ study to ascertain the utility of **1** dissolved in Exxal-8 at higher acid concentrations (Figure 2b).

As delineated, the extraction of $^{241}Am^{3+}$ from the acidic aqueous phase to the organic phase was more efficient at increasing $HNO_{3(aq)}$ concentrations, in opposition to contemporary BTPs. Complete extraction of $^{241}Am^{3+}$ was not realized in Exxal-8, although extraction approached 81%. The percent extraction of $^{241}Am^{3+}$ in the organic phase, which was benchmarked to the initial counts per minute (CPM), increased from 38% at 0.25 M $HNO_{3(aq)}$ to 59% at 0.50 $HNO_{3(aq)}$ to as high as 81% at 5 M $HNO_{3(aq)}$. A $S_{F(Am/Eu)}$ > 100 was observed at all acid concentrations. D_{Eu} resulted in a comparable trend to D_{Am}, where an increase in distribution was observed as a function of increasing acid concentration, with the largest D_{Eu} observed at 5 M $HNO_{3(aq)}$ corresponding to a 5% extraction of $^{154}Eu^{3+}$ based on initial CPM.

Additional experimentation evaluated the D_{Am} effect at 1 M $HNO_{3(aq)}$ as a function of [**1**] (Figure 2c). A series of experiments which varied the concentration of **1** while maintaining constant $[HNO_{3(aq)}]$ at 1 M for a 60 min contact time were performed, resulting in higher observed D_{Am} and D_{Eu} as a function of the increased concentration of **1**. An error-weighted linear regression was performed, resulting in a slope of the log−log plot of 2.08 ± 0.12 (Figure 2 (d)) for $^{241}Am^{3+}$ and suggesting a 2:1 ligand−metal complex (eq 3). The extraction of $^{154}Eu^{3+}$ was not detected (i.e., the net CPM of the organic phase were below the critical limit) until the concentration of **1** reached 25 mM, thereby supporting minimal $^{154}Eu^{3+}$ extraction.

$$^{241}Am^{3+}_{(aq)} + 3NO_3^- + n\vec{\mathbf{1}} \leftrightarrow [^{241}Am(NO_3)_3(\mathbf{1})_{1-2}]_{(org)} \quad (3)$$

Complexants displaying high affinity for the minor An over Ln frequently bind the former so tightly that the ability to modulate $[HNO_3]$ for the purposes of An deposition in the aqueous phase for decomplexation to complete the separation cycle often requires the use of competitive decomplexation or stripping agents. Interested in ascertaining the feasibility of An^{3+} stripping from complexed $^{241}Am^{3+}$ with **1**, conditions were explored leading to the results delineated in Figure 3a,b below.

An initial separation experiment of **1** in Exxal-8 (25 mM) and 5 M $HNO_{3(aq)}$ was performed to load the organic phase with complexed ^{241}Am. The data observed in Figure 3a correlated $^{241}Am^{3+}$ activity (CPM) of the loaded organic phase after the initial extraction of $^{241}Am^{3+}$ in 5 M HNO_3 (Figure 3a, red) following the standard separation experiment described in Figure 2c and $^{241}Am^{3+}$ activity (CPM) of the decomplexed organic phase after 60 min contact time with an inactive aqueous phase of $[HNO_{3(aq)}]$ at 1.00 × 10^{-3}−1.00 × 10^{-1} M (Figure 3a, blue). When the $[HNO_{3(aq)}]$ reached 10 mM, 26.3% of the bound $^{241}Am^{3+}$ had transitioned from the Exxal-8 organic phase to the aqueous phase, thereby demonstrating proof of principle regarding the potential for An decomplexation, most notably without phase modification or competitive ligand exchange to facilitate placement of the An back in the aqueous phase.

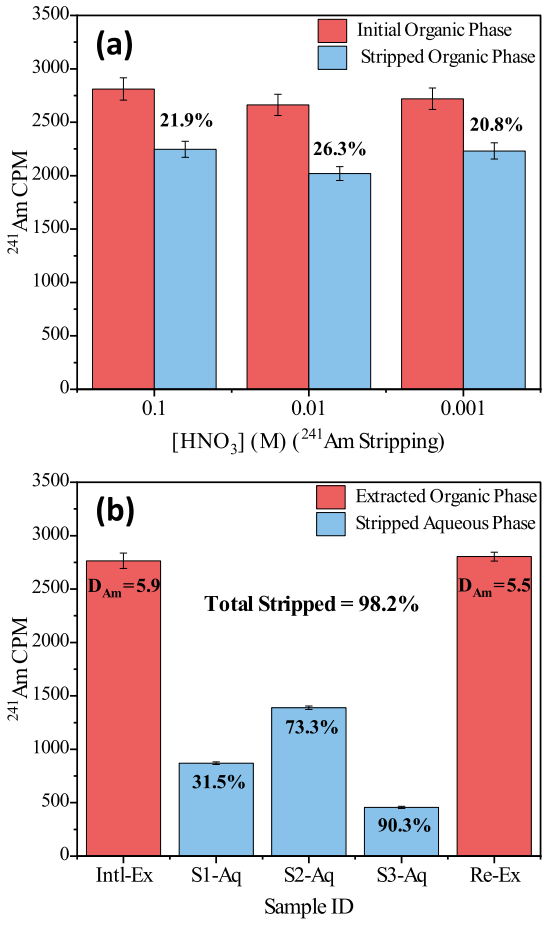

Figure 3. (a) Extraction and Decomplexation of $^{241}Am^{3+}$ Studies in Exxal-8 at Various $[HNO_{3(aq)}]$, Complexant **1** (25 mM) dissolved in Exxal-8 as the organic phase, $^{241}Am^{3+}$ and $^{154}Eu^{3+}$ tracers, and 4 M $HNO_{3(aq)}$ prior to contact with the organic phase. The initial concentration of $HNO_{3(aq)}$ varied from 1.00 × 10^{-3}−1.00 × 10^{-1} M and (b) extraction and decomplexation of $^{241}Am^{3+}$ in Exxal-8 at 10 mM $HNO_{3(aq)}$ for three successive decomplexations, followed by $^{241}Am^{3+}$ re-extraction with the original complexant.

The results in Figure 3a substantiated 10 mM as the slightly preferred $HNO_{3(aq)}$ concentration, and a second decomplexation study was performed to determine if additional $^{241}Am^{3+}$ could be decomplexed with subsequent additions of fresh $HNO_{3(aq)}$ and if **1** could be recycled for an additional extraction (Figure 3b). Each additional aqueous phase was added in equal volume to the organic phase and contacted for 60 min. The results revealed that a total of 98.2% of the initial $^{241}Am^{3+}$ extracted from the initial organic phase was decomplexed within three washes with 10 mM $HNO_{3(aq)}$. Complexant **1** was able to be recycled for a second extraction

https://doi.org/10.1021/acs.inorgchem.3c02061
Inorg. Chem. 2024, 63, 4819−4827

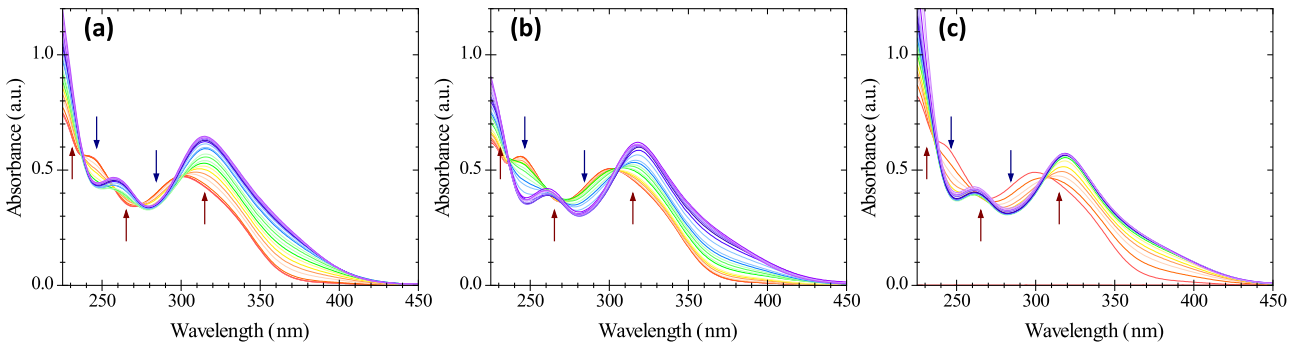

Figure 4. (a) UV−vis spectra of **1** upon the addition of $Nd(NO_3)_3$. Solvent system 99% acetonitrile/1% water (v/v). [**1**] = 1.5×10^{-5} M, [$Nd(NO_3)_3$] = 7.5×10^{-7} to 4.5×10^{-5} M, (b) UV−vis Spectra of **1** upon addition of $Eu(NO_3)_3$. Solvent system 99% acetonitrile/1% water (v/v) solvent system. [**1**] = 1.5×10^{-5} M, [$Eu(NO_3)_3$] = 7.5×10^{-7} to 4.5×10^{-5} M, and (c) UV−vis Spectra of **1** upon addition of $Ho(NO_3)_3$. Solvent system 99% acetonitrile/1% water (v/v) solvent system. [**1**] = 1.5×10^{-5} M, [$Ho(NO_3)_3$] = 7.5×10^{-7} to 4.5×10^{-5} M.

with comparable D_{Am} values of 5.9 and 5.5 for the initial and second extractions, respectively.

In summary, separation of $^{241}Am^{3+}$ with **1** from a biphasic system via liquid−liquid extraction was productive, and the separation cycle for this system could be completed with a high degree of efficacy via decomplexation experiments in Exxal-8.

At the conclusion of liquid−liquid separation experiments, research focus shifted toward spectroscopic measurements of the unbound complexant as well as the bound metal/ligand complex with Nd^{3+}, Eu^{3+}, and Ho^{3+} as cold Ln surrogates (early, middle, and late) to $^{241}Am^{3+}$, in addition to measuring their stability constants, log β.[24,25]

Spectroscopic Measurements. UV−visible spectrometric titrations with **1** were initiated to investigate the complexation behavior with $Ln(NO_3)_3$, Nd^{3+} (Figure 4a), Eu^{3+} (Figure 4b), and Ho^{3+} (Figure 4c) in a 99:1 CH_3CN/H_2O (v/v) solution.[26] By monitoring the change in UV−vis spectra of **1** titrated with Ln^{3+}, the metal−ligand complexation can be detected. HypSpec software was leveraged to evaluate the spectra and calculate the associated stability constants of each Ln^{3+} species.

Absorbance peaks of free (uncomplexed) **1** (red line) appear at 245 and 303 nm. Upon addition of $Ln(NO_3)_3$, the peaks displayed bathochromic shifts to 260 and 316 nm, respectively.

The pattern in the spectral shifts was common for each Ln^{3+} analyzed (Figure 4a−c). A lack of well-defined isosbestic points indicated the presence of more than two species in solution with overlapping but distinct absorption spectra.

Factor analysis of the spectra in HypSpec implicated five significant factors for Nd^{3+} and Eu^{3+} and four for Ho^{3+}.[27] In each case, the final factor displayed excessive noise in the eigenvector plot, and its singular value was well below unity (10^{-2} to 10^{-3}) and, therefore, was excluded from the model. Initial models were run with consideration of two complexes, ML and ML2, and successfully returned the best fits for all spectra.[28] A third complex, ML3, was added to the model, and a best fit was obtained for Nd^{3+} and Eu^{3+}. However, the model convergence failed for Ho^{3+}. This result supported the factor analysis, where one extra factor was observed for Nd^{3+} and Eu^{3+}. The calculated stability constants are displayed in Table 1. An increase in the stability constants was observed from Nd^{3+} to Eu^{3+}, and a decrease was noted for Ho^{3+}. This bell-shaped variation along the Ln series has been observed by other N-donor BTP ligands.[29]

Single-Crystal X-ray Crystallography. Successful crystal formation was secured via a vapor deposition experiment of **1** with $Nd(NO_3)_3$, resulting in crystals of a suitable polymorph which were effectively studied by SC-XRD (Figure 5). These results revealed that the metal was stabilized by two inner and one outer sphere interactions with NO_3^- anions in the crystal structure. The Nd^{3+} center was bound to two discrete ligands of **1** (Table 2). Although direct correlation between the solid state and solution phase bond angles of the bound metal−ligand complex is not always commensurate,[30] a working hypothesis was that the edge-π stacking of the 5,6-diaryl rings and extended alkoxy side chains impacted the necessary molecular topography to accentuate the solubility of the free ligand and bound metal−ligand complex in the diluent evaluated. The outer sphere NO_3^- interaction suggested that

Table 1. Stability Constants (log β) for the Formation of Nd(III), Eu(III), and Ho(III) Complexes with 1(L) at 298 ± 1 K

metal	reaction	log β
Nd^{3+}	$L + Nd^{3+} \rightleftharpoons NdL^{3+}$	6.98 ± 0.02
	$2\ L + Nd^{3+} \rightleftharpoons NdL_2^{3+}$	12.75 ± 0.03
	$3\ L + Nd^{3+} \rightleftharpoons NdL_3^{3+}$	16.60 ± 0.07
Eu^{3+}	$L + Eu^{3+} \rightleftharpoons EuL^{3+}$	7.68 ± 0.02
	$2\ L + Eu^{3+} \rightleftharpoons EuL_2^{3+}$	13.50 ± 0.03
	$3\ L + Eu^{3+} \rightleftharpoons EuL_3^{3+}$	18.80 ± 0.07
Ho^{3+}	$L + Ho^{3+} \rightleftharpoons HoL^{3+}$	5.90 ± 0.05
	$2\ L + Ho^{3+} \rightleftharpoons HoL_2^{3+}$	11.40 ± 0.06

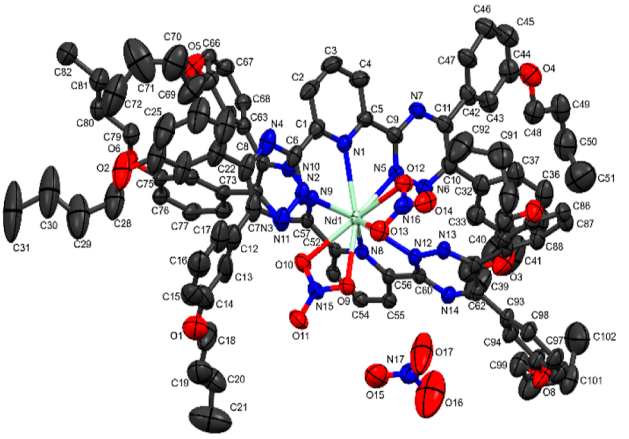

Figure 5. Single-crystal X-ray diffraction of the $Nd(NO_3)_3$ 3,3′-butyloxy BTP complex at the 50% probability level.

https://doi.org/10.1021/acs.inorgchem.3c02061
Inorg. Chem. 2024, 63, 4819−4827

Table 2. Single-Crystal X-ray Crystallographic Data and Refinement Parameters for $[Nd(1)_2(NO_3^-)_3]$

parameter	data
empirical formula	$C_{102}H_{110}N_{17}NdO_{17}$
CCDC number	2267981
formula weight	1990.30
temperature/K	120(2)
crystal system	triclinic
space group	$P\bar{1}$
wavelength	1.54178 Å
unit cell dimensions	a = 16.6761(17) Å
	b = 17.2185(13) Å
	c = 17.7859(16) Å
	α = 100.076(4)°
	β = 102.773(5)°
	γ = 92.110(5)°
volume	4888.6(8) Å^3
Z	2
density (calculated)	1.352 g.cm^{-3}
absorption coefficient (μ)	4.670 mm^{-1}
F(000)	2074
crystal color, habit	orange, tablet
crystal size	0.108 × 0.089 × 0.018 mm^3
θ range for data collection	2.593 to 72.941°
index ranges	$-20 \le h \le 20$, $-21 \le k \le 21$, $-17 \le l \le 22$
reflections collected	121,215
independent reflections	19,352 [R_{int} = 0.1081]
completeness to θ = 67.679°	100.0%
absorption correction	Numerical
max. and min transmission	0.7668 and 0.53
refinement method	full-matrix least-squares on F^2
data/restraints/parameters	19352/72/1280
goodness-of-fit on F^2	1.031
final R indices [$I > 2\sigma(I)$]	R_1 = 0.0626, wR_2 = 0.1581
R indices (all data)	R_1 = 0.0743, wR_2 = 0.1660
extinction coefficient	n/a
largest diff. peak and hole	1.317 and −0.994 e$^-$·Å^{-3}

ligand back-bonding may assist in stabilizing the charge of Nd^{3+} such that only two NO_3^- ions are required in the inner coordination sphere in the solid state but three overall to balance total charge (Figure 5).

DFT Calculations. The atomic coordinates obtained from the SC-XRD data were used for the initial structural minimizations for DFT. Geometry optimizations to further refine structures for the $M^{3+}(\mathbf{1})_2$ complexes with $^{241}Am^{3+}$ (Figure 6) underscored the integration of experimental results obtained from synthesis and separations with computational methods. The topography of the DFT-minimized complex reinforced the concept of bipolar complexation, whereby the hydrophobic alkyl groups adjacent to the aromatic substituents at the 5,6-position of the 1,2,4-triazine facilitated more favorable interaction with the nonpolar diluent, Exxal-8, whereas the polar N-core set up well for selective chelation of $^{241}Am^{3+}$.

The complexation of $^{154}Eu^{3+}$ and $^{241}Am^{3+}$ with the complexants **1** (one or two complexants per metal) and H_2O or NO_3^- to complete the inner coordination sphere was studied using DFT[31] with the hybrid B3LYP functional[32] in conjunction with the 28($^{154}Eu^{3+}$) and 60($^{241}Am^{3+}$) core electron Stuttgart effective core potentials (ECP) and corresponding basis sets.[33] The DFT-optimized DZVP2[34]

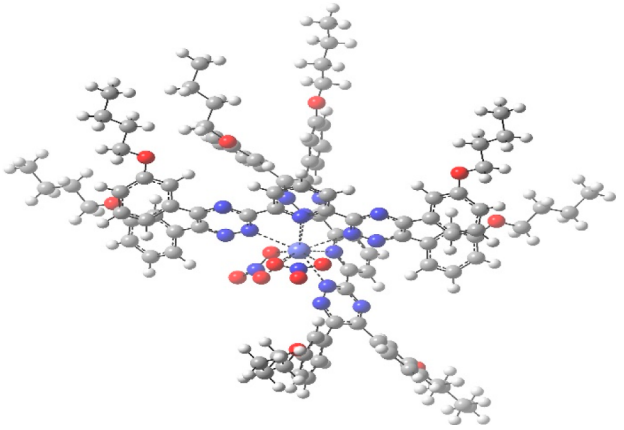

Figure 6. DFT geometry optimized structure of the $^{241}Am(NO_3)_3$-3,3′-butyloxy BTP complex.

basis set was used for H, C, N, and O. This combination of DFT functionals and basis sets/ECPs has been demonstrated to work well previously.[35] Gas phase-free energies were assessed by using vibrational frequency calculations, which were subsequently incorporated in solvation calculations. The quasiharmonic approximation from Truhlar and co-workers was employed to correct the entropy associated with low-frequency vibrational modes; these are numerous in such large, sterically crowded structures. In this approach, all harmonic frequencies below 100 cm^{-1} were raised to 100 cm^{-1} before evaluation of the vibrational component for entropy.[36] Solvent effects were treated using a self-consistent reaction field[37] with the conductor-like screening model (COSMO).[38] Default Klamt radii[39] were used for all atoms, except the f-block elements. The solvation radii used for $^{154}Eu^{3+}$ and $^{241}Am^{3+}$ were 2.007 and 2.205 Å, respectively. Solvents were chosen as representative of the aqueous and organic phases of the liquid−liquid extraction described above.[40] The ΔG_{Rxn} in solution (ΔG_{sol}) complexation energy was calculated as the sum of the gas phase free energy (ΔG_{gas}) and the ΔG due to the solvent determined from the COSMO calculation (ΔG_{solv}) in eq 4.

$$\Delta G_{sol} = \Delta G_{gas} + \Delta G_{solv} \tag{4}$$

Previous work, validated by Extended X-ray Absorption Fine Structure (EXAFS) and Raman spectroscopy measurements, has shown that nine is an appropriate coordination number for aqueous f-block elements, although Eu(III) can have coordination numbers (CN) from 8 to 9.[41] To ensure a consistent comparison, CN = 9 was selected for the hydrated metal ion for both $^{154}Eu^{3+}$ and $^{241}Am^{3+}$. Several reactions were explored to gain insight into the stability of the resulting metal−ligand complexes. The separation factors were obtained from Reaction 1 for the monocomplexant case with five H_2O, Reaction 2 for the dicomplexant case (supported by UV−visible spectroscopic and separation studies) with two H_2O molecules, and Reaction 3 for the dicomplexant case with two nitrates (supported by SC-XRD and separation studies).

$$[M(H_2O)_9]^{3+}_{+}[\acute{M}L(H_2O)_5]^{3+} \rightarrow [\acute{M}(H_2O)_9]^{3+} + [ML(H_2O)_5]^{3+} \tag{R1}$$

https://doi.org/10.1021/acs.inorgchem.3c02061
Inorg. Chem. 2024, 63, 4819−4827

Table 3. Comparative Analysis of 1 with Various Hydration and Complexant/Metal Ratios

M → Ḿ	$K_{eq,aq}$	$K_{eq,but}$	$K_{eq,aq}$	$K_{eq,but}$	$K_{eq,aq}$	$K_{eq,but}$
	Reaction R1		Reaction R2		Reaction R3	
Am → Eu	7.2	3.6	1.4×10^{-3}	2.1×10^{-3}	3.5×10^{-2}	3.6×10^{-2}

$$[\acute{M}(H_2O)_9]^{3+} + [ML_2(H_2O)_2]^{3+} \rightarrow [M(H_2O)_9]^{3+} + [\acute{M}L_2(H_2O)_2]^{3+} \quad (R2)$$

$$[\acute{M}(H_2O)_9]^{3+} + [ML_2(NO_3)_2]^{+} \rightarrow [M(H_2O)_9]^{3+} + [\acute{M}L_2(NO_3)_2]^{+} \quad (R3)$$

The results in Table 3 demonstrated that when five H_2O are present in the inner coordination sphere for the mono-complexant with (**1**), $^{154}Eu^{3+}$ is preferred over $^{241}Am^{3+}$, in contrast to the experiment, which results in the opposite observation. When two complexants are present, $^{241}Am^{3+}$ is clearly preferred over $^{154}Eu^{3+}$ independent of whether there is an H_2O or NO_3^- counterion in the first solvation shell. When one complexant is present with multiple H_2O molecules, charge transfer between $^{154}Eu^{3+}$ and the complexant is predicted, resulting in a redox process to generate Eu^{2+} and an oxidized complexant with $^{154}Eu^{3+}$ having an f^7 configuration. The presence of the additional complexant, or NO_3^-, stabilizes the charge (+3) on the Eu, so no charge transfer occurs. Thus, the coordination shell of the cation can impact selectivity and needs to be further explored.

CONCLUSIONS

In summary, the solubility of **1** in Exxal-8 was a first for an aryl-substituted BTP. The incorporation of hydrocarbon functionality along the aromatic backbone of the complexant allowed for improved solubility and performance. The robust stability of the complexant to hydrolytic degradation was usurped only by the outstanding performance in separating the minor An $^{241}Am^{3+}$ from $^{154}Eu^{3+}$ from simulated SNF with high *D* values and *SF*. Recovery of the separated An through decomplexation studies and subsequent comparable recycled extraction furthered the understanding of minor An separations from Ln in biphasic systems. Crystallographic analysis of the metal/ligand complex implied a high degree of ligand back-bonding in the case of lanthanides, resulting in two inner and one outer sphere anion interactions, while spectroscopic experiments highlighted complex properties with various Ln^{3+}. DFT calculations showed that if only water is present in the inner coordination sphere, Eu(III) is favored over Am(III) due to a metal−ligand redox process to generate Eu(II). When nitrates or a second ligand are present, the metal−ligand redox process is shut down, and Am(III) is preferred over Eu(III). Application of this new class of BTP complexants to the separation of other relevant An, including Cm, Bk, cf., and Es, is ongoing and will be reported in due course.

ASSOCIATED CONTENT

Data Availability Statement

The data underlying this study are available in the online Supporting Information.

Supporting Information

The Supporting Information is available free of charge at https://pubs.acs.org/doi/10.1021/acs.inorgchem.3c02061.

Raw data for separations and spectroscopic studies, statistical analysis, single-crystal X-ray diffraction data, and copies of ^1H and ^{13}C NMR spectra for new compounds (PDF)

Accession Codes

CCDC 2267981 contains the supplementary crystallographic data for this paper. These data can be obtained free of charge via www.ccdc.cam.ac.uk/data_request/cif, or by emailing data_request@ccdc.cam.ac.uk, or by contacting The Cambridge Crystallographic Data Centre, 12 Union Road, Cambridge CB2 1EZ, UK; fax: +44 1223 336033.

AUTHOR INFORMATION

Corresponding Author

Jesse D. Carrick − *Department of Chemistry, Tennessee Technological University, Cookeville, Tennessee 38505-0001, United States;* orcid.org/0000-0002-0663-2426; Email: jcarrick@tntech.edu

Authors

Lesta S. Fletcher − *Department of Chemistry, Tennessee Technological University, Cookeville, Tennessee 38505-0001, United States;* orcid.org/0000-0003-2185-848X

Mariah L. Tedder − *Department of Chemistry, Tennessee Technological University, Cookeville, Tennessee 38505-0001, United States*

Samiat O. Olayiwola − *Department of Chemistry, Tennessee Technological University, Cookeville, Tennessee 38505-0001, United States*

Nickolas A. Joyner − *Department of Chemistry, The University of Alabama, Tuscaloosa, Alabama 35487, United States*

Marcos M. Mason − *Department of Chemistry, The University of Alabama, Tuscaloosa, Alabama 35487, United States*

Allen G. Oliver − *Department of Chemistry, The University of Notre Dame, Notre Dame, Indiana 46656, United States;* orcid.org/0000-0002-0511-1127

Dale D. Ensor − *Department of Chemistry, Tennessee Technological University, Cookeville, Tennessee 38505-0001, United States*

David A. Dixon − *Department of Chemistry, The University of Alabama, Tuscaloosa, Alabama 35487, United States;* orcid.org/0000-0002-9492-0056

Complete contact information is available at: https://pubs.acs.org/10.1021/acs.inorgchem.3c02061

Notes

The authors declare no competing financial interest.

ACKNOWLEDGMENTS

Financial support for this work was provided by an award from the U.S. Department of Energy, Basic Energy Sciences, Separations Program, Award: DE-SC0018033. The Camille and Henry Dreyfus Foundation is gratefully acknowledged for a Henry Dreyfus Teacher-Scholar Award to J.D.C. An award from the National Science Foundation Major Research

Instrumentation (MRI) Program (1531870) supported the acquisition of TN Tech's 500 MHz multinuclear NMR spectrometer. Funding for the Bruker Venture X-ray spectrometer at The University of Notre Dame leveraged to acquire single-crystal X-ray crystallographic data was supported by NSF MRI Award CHE-2214606. The authors would like to thank Prof. David Dan, TN Tech, for helpful discussions regarding the radiochemistry experimental technique.

REFERENCES

(1) (a) Lewis, F. W.; Harwood, L. M.; Hudson, M. J.; Afsar, A.; Laventine, D. M.; Šťastná, K.; John, J.; Distler, P. Separation of the Minor Actinides Americium(III) and Curium(III) by Hydrophobic and Hydrophilic BTPhen Ligands: Exploiting Differences in their Rates of Extraction and Effective Separations at Equilibrium. *Solvent Extr. Ion Exch.* **2018**, *36*, 115−135. (b) Bhattacharyya, A.; Ansari, S. A.; Karthikeyan, N. S.; Ravichandran, C.; Venkatachalapathy, B.; Rao, T. S.; Seshadri, H.; Mohapatra, P. K. Bis-(1,2,4-triazin-3-yl) Ligand Structure Driven Selectivity Reversal Between Am^{3+} and Cm^{3+}: Solvent Extraction and DFT Studies. *Dalton Trans.* **2021**, *50*, 7783−7790.

(2) (a) Kolarik, Z. Complexation and Separation of Lanthanides(III) and Actinides(III) by Heterocyclic N-Donors in Solutions. *Chem. Rev.* **2008**, *108*, 4208−4252. (b) Panak, P. J.; Geist, A. Complexation and Extraction of Trivalent Actinides and Lanthanides by Triazinylpyridine N-Donor Ligands. *Chem. Rev.* **2013**, *113*, 1199−1236.

(3) Zsabka, P.; Wilden, A.; Van Hecke, K.; Modolo, G.; Verwerft, M.; Cardinaels, T. Beyond U/Pu Separation: Separation of Americium from the Highly Active PUREX Raffinate. *J. Nucl. Mater.* **2023**, *581*, 154445.

(4) (a) Kolarik, Z.; Müllich, U.; Gassner, F. Selective Extraction of Am(III) over Eu(III) by 2,6-ditriazolyl- and 2,6-ditriazinylpyridines. *Solvent Extr. Ion Exch.* **1999**, *17*, 23−32. (b) Kolarik, Z.; Müllich, U.; Gassner, F. Extraction of Am(III) and Eu(III) Nitrates by 2,6-di(5,6)-dipropyl-1,2,4-triazin-3-yl)pyridine. *Solvent Extr. Ion Exch.* **1999**, *17*, 1155−1183. (c) Case, F. H. The Preparation of Hydrazidines and as-Triazines Related to Substituted 2-Cyanopyridines. *J. Org. Chem.* **1965**, *30*, 931−933.

(5) Trumm, M.; Schimmelpfennig, B. Towards the Origin of Effective An(III)/Ln(III) Separation by Tridentate N-donor Ligands: A Theoretical Study on Atomic Charges and Polarisabilities for Cm(III)/Gd(III) Separation. *Mol. Phys.* **2016**, *114*, 876−883.

(6) (a) Maiwald, M. M.; Wagner, A. T.; Kratsch, J.; Skerencak-Frech, A.; Trumm, M.; Geist, A.; Roesky, P. W.; Panak, P. J. 4,4'-Di-tert-butyl-6-(1H-tetrazol-5-yl)-2,2'-bipyridine: Modification of a Highly Selective N-donor Ligand for the Separation of Trivalent Actinides from Lanthanides. *Dalton Trans.* **2017**, *46*, 9981−9994. (b) Hubscher-Bruder, V.; Haddaoui, J.; Bouhroum, S.; Arnaud-Neu, F. Recognition of Some Lanthanides, Actinides, and Transition- and Heavy-Metal Cations by N-Donor Ligands: Thermodynamic and Kinetic Aspects. *Inorg. Chem.* **2010**, *49*, 1363−1371. (c) Lan, J.-H.; Shi, W.-Q.; Yuan, L.-Y.; Zhao, Y.-L.; Li, J.; Chai, Z.-F. Trivalent Actinide and Lanthanide Separations by Tetradentate Nitrogen Ligands: A Quantum Chemistry Study. *Inorg. Chem.* **2011**, *50*, 9230−9237. (d) Waters, G. D.; Carrick, J. D. Convergent Access to bis-1,2,4-triazinyl-2,2'-bipyridines (BTBPs) and 2,2'-bipyridines via a Pd-catalyzed Ullman-type reaction. *RSC Adv.* **2020**, *10*, 10807−10815.

(7) (a) Lewis, F. W.; Harwood, L. M.; Hudson, M. J.; Drew, M. G. B.; Desreux, J. F.; Vidick, G.; Bouslimani, N.; Modolo, G.; Wilden, A.; Sypula, M.; Vu, T.-H.; Simonin, J.-P. Highly Efficient Separation of Actinides from Lanthanides by a Phenanthroline-Derived Bis-Triazine Ligand. *J. Am. Chem. Soc.* **2011**, *133*, 13093−13102. (b) Zsabka, P.; Opsomer, T.; Van Hecke, K.; Dehaen, W.; Wilden, A.; Modolo, G.; Verwerft, M.; Binnemans, K.; Cardinaels, T. Solvent Extraction Studies for the Separation of Trivalent Actinides from Lanthanides with a Triazole-functionalized 1,10-phenanthroline Extractant. *Solvent Extr. Ion Exch.* **2020**, *38*, 719−734.

(8) Zaytsev, A. V.; Bulmer, R.; Kozhevnikov, V. N.; Sims, M.; Modolo, G.; Wilden, A.; Waddell, P. G.; Geist, A.; Panak, P. J.; Wessling, P.; Lewis, F. W. Exploring the Subtle Effect of Aliphatic Ring Size on Minor Actinide-Extraction Properties and Metal Ion Speciation in Bis-1,2,4-Triazine Ligands. *Chem.—Eur. J.* **2020**, *26*, 428−437.

(9) (a) Weßling, P.; Maag, M.; Baruth, G.; Sittel, T.; Sauerwein, F. S.; Wilden, A.; Modolo, G.; Geist, A.; Panak, P. J.; Panak, P. Complexation and Extraction Studies of Trivalent Actinides and Lanthanides with Water-Soluble and CHON-Compatible Ligands for the Selective Extraction of Americium. *Inorg. Chem.* **2022**, *61*, 17719−17729. (b) Bhattacharyya, A.; Ansari, S. A.; Prabhu, D. R.; Kumar, D.; Mohapatra, P. K. Highly Efficient Separation of Am^{3+} and Eu^{3+} using an Aqueous Soluble Sulfonated BTP Derivative by Hollow-Fiber Supported Liquid Membrane Containing TODGA. *Sep. Sci. Technol.* **2019**, *54*, 1512−1520. (c) Geist, A.; Müllich, U.; Magnusson, D.; Kaden, P.; Modolo, G.; Wilden, A.; Zevaco, T. Actinide(III)/Lanthanide(III) Separation via Selective Aqueous Complexation of Actinides(III) using a Hydrophilic 2,6-Bis(1,2,4-Triazin-3-yl)-pyridine in Nitric Acid. *Solvent Extr. Ion Exch.* **2012**, *30*, 433−444. (d) Ruff, C. M.; Müllich, U.; Geist, A.; Panak, P. J. Complexation of Cm(III) and Eu(III) with a Hydrophilic 2,6-Bis(1,2,4-triazin-3-yl)-pyridine Studied by Time-Resolved Laser Fluorescence Spectroscopy. *Dalton Trans.* **2012**, *41*, 14594−14602.

(10) Bhattacharyya, A.; Ansari, S. A.; Karthikeyan, N. S.; Ravichandran, C.; Venkatachalapathy, B.; Rao, T. S.; Seshadri, H.; Mohapatra, P. K. Bis-(1,2,4-triazin-3-yl) Ligand Structure Driven Selectivity Reversal Between Am^{3+} and Cm^{3+}: Solvent Extraction and DFT Studies. *Dalton Trans.* **2021**, *50*, 7783−7790.

(11) (a) Mahmoud, J.; Higginson, M.; Thompson, P.; Gilligan, C.; Livens, F.; Scott, H. Rapid Separation of Americium from Complex Matrices using Solvent Impregnated Triazine Extraction Chromatography Resins. *J. Chromatogr. A* **2022**, *1669*, 462950. (b) Afsar, A.; Distler, P.; Harwood, L. M.; John, J.; Westwood, J. Extraction of Minor Actinides, Lanthanides, and Other Fission Products by Silica-Immobilized BTBP/BTPhen Ligands. *Chem. Commun.* **2017**, *53*, 4010−4013.

(12) (a) Tai, S.; Williams, N. J.; Carrick, J. D. Synthesis of *bis*-1,2,4-triazines via Telescoped Condensation of [1,10]-phenanthroline-2,9-dicarbonitrile with Aromatic 1,2-Dicarbonyls. *J. Heterocycl. Chem.* **2016**, *53*, 307−312. (b) Tai, S.; Marchi, S. V.; Carrick, J. D. Efficient Preparation of Pyridinyl-1,2,4-triazines via Telescoped Condensation with Diversely Functionalized 1,2-dicarbonyls. *J. Heterocycl. Chem.* **2016**, *53*, 1138−1146.

(13) (a) Tai, S.; Dover, E. J.; Marchi, S. V.; Carrick, J. D. Pd-Catalyzed Diamination of 1,2,4-Triazinyl Complexant Scaffolds. *J. Org. Chem.* **2015**, *80*, 6275−6282. (b) Cleveland, J. W.; Carrick, J. D. Pd-Catalyzed Amination of Functionalized 6-Bromo-pyridinyl-1,2,4-triazine Complexant scaffolds. *Eur. J. Org Chem.* **2017**, *2017*, 3318−3327.

(14) Chin, A.-L.; Carrick, J. D. Modular Approaches to Diversified Soft Lewis Basic Complexants through Suzuki-Miyaura Cross-Coupling of Bromoheteroarenes with Organotrifluoroborates. *J. Org. Chem.* **2016**, *81*, 1106−1115.

(15) (a) Dzeagu, F. O.; Carrick, J. D. Synthetic Access to Unsymmetric, Tridentate, Pyridyl-1,3,4-oxadiazole Complexants via Intramolecular Oxidative Annulation of Arylhydrazides with Heteroaryl Carbaldehydes. *J. Org. Chem.* **2023**, *88*, 419−432. (b) Gulledge, Z. Z.; Duda, D. P.; Dixon, D. A.; Carrick, J. D. Microwave-Assisted, Metal- and Azide-Free Synthesis of Functionalized Heteroaryl-1,2,3-triazoles via Oxidative Cyclization of N-Tosylhydrazones and Anilines. *J. Org. Chem.* **2022**, *87*, 12632−12643. (c) Guillet, G. L.; Hyatt, I. F. D.; Hillesheim, P. C.; Abboud, K. A.; Scott, M. J. 1,2,4-Triazine-picolinamide Functionalized Nonadentate Chelates for the Segregation of Lanthanides(III) and Actinides(III) in Biphasic Systems. *New J. Chem.* **2013**, *37*, 119−131.

(16) (a) Gulledge, Z. Z.; Tedder, M. L.; Lyons, K. R.; Carrick, J. D. Synthesis of Tridentate [1,2,4] Triazinyl-Pyridin-2-yl Indole Lewis Basic Complexants via Pd-Catalyzed Suzuki−Miyaura Cross-Cou-

https://doi.org/10.1021/acs.inorgchem.3c02061
Inorg. Chem. 2024, 63, 4819−4827

pling. *ACS Omega* **2019**, *4*, 18855−18866. (b) Veerakanellore, G. B.; Smith, C. M.; Vasiliu, M.; Oliver, A. G.; Dixon, D. A.; Carrick, J. D. Synthesis of 1H-pyrazol-5-yl-pyridin-2-yl-[1,2,4]triazinyl Soft-Lewis Basic Complexants via Metal and Oxidant Free [3 + 2] Dipolar Cycloaddition of Terminal Ethynyl Pyridines with Tosylhydrazides. *J. Org. Chem.* **2019**, *84*, 14558−14570.

(17) Mason, M. M.; Smith, C. M.; Vasiliu, M.; Carrick, J. D.; Dixon, D. A. Prediction of An(III)/Ln(III) Separation by 1,2,4-Triazinylpyridine Derivatives. *J. Phys. Chem. A* **2021**, *125*, 6529−6542.

(18) Xia, M.; Yang, X.; Chai, Z.; Wang, D. Stronger Hydration of Eu(III) Impedes Its Competition against Am(III) in Binding with N-donor Extractants. *Inorg. Chem.* **2020**, *59*, 6267−6278.

(19) (a) Hill, T. G.; Chin, A.-L.; Tai, S.; Carrick, J. D.; Ensor, D. D.; Delmau, L. H. Separation of Americium from Europium using 3,3′-Dimethoxy-phenyl-bis-1,2,4-triazinyl-2,6-pyridine. *Sep. Sci. Technol.* **2018**, *53*, 1848−1855. (b) Ebenezer, C.; Solomon, R. V. Insights into the Extraction of Actinides from Lanthanides using 3,3′-Dimethoxy-phenyl-bis-1,2,4-triazinyl-2,6-pyridine Ligand-A DFT Study. *Chem. Select* **2020**, *5*, 13895−13901. (c) Dupont, C.; Hill, C.; Suzenet, F.; Guillaumet, G. Influence of an Alkoxy Group on Bis-Triazinyl-Pyridines for Selective Extraction of Americium(III). *Solvent Extr. Ion Exch.* **2013**, *31*, 253−268.

(20) (a) Trumm, S.; Geist, A.; Panak, P. J.; Fanghänel, T. An Improved Hydrolytically-Stable Bis-Triazinyl-Pyridine (BTP) for Selective Actinide Extraction. *Solvent Extr. Ion Exch.* **2011**, *29*, 213−229. (b) Tevepaugh, K. N.; Coonce, J. G.; Tai, S.; Delmau, L. H.; Carrick, J. D.; Ensor, D. D. Chromatographic Separation of Americium from Europium using *bis*-2,6-(5,6,7,8-tetrahydro-5,9,9-trimethyl-5,8-methano-1,2,4-benzotriazin-3-yl) Pyridine. *J. Radioanal. Nucl. Chem.* **2017**, *314* (1), 371−376.

(21) Previous reports describe the impact of BTPs with a 4-methoxy substituent compared to the methyl substituted derivative on Am/Eu separations Dupont, C.; Hill, C.; Suzenet, F.; Guillaumet, G. Influence of an Alkoxy Group on Bis-Triazinyl-Pyridines for Selective Extraction of Americium(III). *Solvent Extr. Ion Exch.* **2013**, *31*, 253−268.

(22) Brand name mixture of branched 8-carbon alcohols produced from olefin hydration sold by Exxon Mobil, Corp.

(23) Tedder, M. L.; Carrick, J. D. A Synthetic Strategy for the Preparation of Alkoxy-Functionalized Bis-1,2,4-triazinyl-pyridines. *J. Heterocycl. Chem.* **2024**, in review.

(24) Please see ref 12.

(25) Mutoh, K.; Miyashita, N.; Arai, K.; Abe, J. Turn-On Mode Fluorescence Switch by using Negative Photochromic Imidazole Dimer. *J. Am. Chem. Soc.* **2019**, *141*, 5650−5654.

(26) (a) Weigl, M.; Geist, A.; Müllich, U.; Gompper, K. Kinetics of Americium(III) Extraction and Back Extraction with BTP. *Solvent Extr. Ion Exch.* **2006**, *24*, 845−860. (b) Miguirditchian, M.; Guillaneux, D.; Francois, N.; Airvault, S.; Ducros, S.; Thauvin, D.; Madic, C.; Illemassène, M.; Lagarde, G.; Krupa, J. C. Complexation of Lanthanide(III) and Actinide(III) Cations with Tridentate Nitrogen-Donor Ligands: A Luminescence and Spectrophotometric Study. *Nucl. Sci. Eng.* **2006**, *153*, 223−232. (c) Rawat, N.; Bhattacharyya, A.; Ghosh, S. K.; Gadly, T.; Tomar, B. S. Thermodynamics of Complexation of Lanthanides with 2,6-bis(5,6-diethyl-1,2,4-triazin-3-yl) pyridine. *Radiochim. Acta* **2011**, *99*, 705−712.

(27) Gans, P.; Sabatini, A.; Vacca, A. Investigation of equilibria in solution. Determination of equilibrium constants with the HYPERQUAD suite of programs. *Talanta* **1996**, *43* (10), 1739−1753.

(28) Galluccio, F.; Macerata, E.; Weßling, P.; Adam, C.; Mossini, E.; Panzeri, W.; Mariani, M.; Mele, A.; Geist, A.; Panak, P. J. Insights into the Complexation Mechanism of a Promising Lipophilic PyTri Ligand for Actinide Partitioning from Spent Nuclear Fuel. *Inorg. Chem.* **2022**, *61*, 18400−18411.

(29) (a) Miguirditchian, M.; Guillaneux, D.; Guillaumont, D.; Moisy, P.; Madic, C.; Jensen, M. P.; Nash, K. L. Thermodynamic Study of the Complexation of Trivalent Actinide and Lanthanide Cations by ADPTZ, a Tridentate N-Donor Ligand. *Inorg. Chem.* **2005**, *44* (5), 1404−1412. (b) Dupont, C.; Hill, C.; Suzenet, F.; Guillaumet, G. Influence of an Alkoxy Group on Bis-Triazinyl-Pyridines for Selective Extraction of Americium(III). *Solvent Extr. Ion Exch.* **2013**, *31* (3), 253−268.

(30) Banik, N. L.; Denecke, M. A.; Geist, A.; Modolo, G.; Panak, P. J.; Rothe, J. 2,6-Bis(5,6-dipropyl-1,2,4-triazin-3-yl)-pyridine: Structures of An(III) and Ln(III) 1:3 Complexes and Selectivity. *Inorg. Chem. Commun.* **2013**, *29*, 172−174.

(31) Parr, R. G.; Yang, W. *Density-Functional Theory of Atoms and Molecules*; Oxford University Press: New York, 1989.

(32) (a) Becke, A. D. Density-Functional Thermochemistry. III. The Role of Exact Exchange. *J. Chem. Phys.* **1993**, *98*, 5648−5652. (b) Lee, C.; Yang, W.; Parr, R. G. Development of the Colle-Salvetti Correlation-Energy Formula into a Functional of the Electron Density. *Phys. Rev. B* **1988**, *37*, 785−789.

(33) (a) Dolg, M.; Stoll, H.; Preuss, H. Energy-Adjusted Ab Initio Pseudopotentials for the Rare Earth Elements. *J. Chem. Phys.* **1989**, *90*, 1730−1734. (b) Cao, X.; Dolg, M. Segmented Contraction Scheme for Small-Core Lanthanide Pseudopotential Basis Sets. *J. Mol. Struct.: THEOCHEM* **2002**, *581*, 139−147. (c) Cao, X.; Dolg, M. Segmented Contraction Scheme for Small-Core Actinide Pseudopotential Basis sets. *J. Mol. Struct.: THEOCHEM* **2004**, *673*, 203−209. (d) Cao, X.; Dolg, M.; Stoll, H. Valence Basis Sets for Relativistic Energy-Consistent Small-Core Actinide Pseudopotentials. *J. Chem. Phys.* **2003**, *118*, 487−496.

(34) Godbout, N.; Salahub, D. R.; Andzelm, J.; Wimmer, E. Optimization of Gaussian-Type Basis Sets for Local Spin Density Functional Calculations. Part I. Boron through Neon, Optimization Technique and Validation. *Can. J. Chem.* **1992**, *70*, 560−571.

(35) (a) Chen, M.; Dixon, D. A.; Wang, X.; Cho, H.; Andrews, L. Matrix Infrared Spectroscopic and Electronic Structure Investigation of the Lanthanide Metal Atom-Methyl Fluoride Reaction Products CH_3-LnF and CH_2-LnHF: The Formation of Single Carbon-Lanthanide Metal Bonds. *J. Phys. Chem. A* **2011**, *115*, 5609−5624. (b) Wang, X.; Cho, H.; Andrews, L.; Chen, M.; Dixon, D. A.; Hu, H.; Li, J. Matrix Infrared Spectroscopic and Computational Investigations of the Lanthanide-Methylene Complexes CH_2LnF_2 with Single Ln-C Bonds. *J. Phys. Chem. A* **2011**, *115*, 1913−1921.

(36) Ribeiro, R. F.; Marenich, A. V.; Cramer, C. J.; Truhlar, D. G. Use of Solution-Phase Vibrational Frequencies in Continuum Models for the Free Energy of Solvation. *J. Phys. Chem. B* **2011**, *115*, 14556−14562.

(37) Tomasi, J.; Mennucci, B.; Cammi, R. Quantum Mechanical Continuum Solvation Models. *Chem. Rev.* **2005**, *105*, 2999−3094.

(38) Klamt, A.; Schüürmann, G. COSMO: A New Approach to Dielectric Screening in Solvents with Explicit Expressions for the Screening Energy and Its Gradient. *J. Chem. Soc., Perkin Trans. 2* **1993**, *5*, 799−805.

(39) Klamt, A. *COSMO-RS: From Quantum Chemistry to Fluid Phase Thermodynamics and Drug Design*; Elsevier: Amsterdam, 2005.

(40) Servis, M. J.; Liu, Z.; Martinez-Baez, E.; Clark, A. E.; Su, J.; Batista, E. R.; Yang, P.; Wildman, A.; Stetina, T.; Li, X.; et al. Solvent Extraction through the Lens of Advanced Modeling and Simulation. In *Ion Exchange and Solvent Extraction*; Moyer, B., Ed.; CRC Press: Boca Raton, FL., 2019; Vol. *5*, pp 147−218.

(41) (a) Knope, K. E.; Soderholm, L. Solution and Solid-State Structural Chemistry of Actinide Hydrates and Their Hydrolysis and Condensation Products. *Chem. Rev.* **2013**, *113*, 944−994. (b) Ohtaki, H.; Radnai, T. Structure and Dynamics of Hydrated Ions. *Chem. Rev.* **1993**, *93*, 1157−1204. (c) Cotton, S. A. Establishing Coordination Numbers for the Lanthanides in Simple Complexes. *C. R. Chim.* **2005**, *8*, 129−145. (d) Ferrier, M. G.; Stein, B. W.; Bone, S. E.; Cary, S. K.; Ditter, A. S.; Kozimor, S. A.; Lezama Pacheco, J. S.; Mocko, V.; Seidler, G. T. The Coordination Chemistry of CmIII, AmIII, and AcIII in Nitrate Solutions: An Actinide L3-Edge EXAFS Study. *Chem. Sci.* **2018**, *9*, 7078−7090.

https://doi.org/10.1021/acs.inorgchem.3c02061
Inorg. Chem. 2024, 63, 4819−4827